Self-Assembled Nanostructure Library from Monodisperse Sequence-Defined Oligo(phosphodiester)s

Donatien de Rochambeau[a], Maciej Barłóg[b], Hassan S. Bazzi[b] and Hanadi F. Sleiman[a*]

a. Department of Chemistry, McGill University, 801, Sherbrooke St. West, Montreal, QC, Canada. H3A 0B8; b. Department of Chemistry, Texas A&M University at Qatar, P.O. Box 23874, Doha, Qatar.

*E-mail: hanadi.sleiman@mcgill.ca

Abstract

Natural biopolymers achieve information storage, molecular recognition and catalysis efficiently through sequence-control. To be able to mimic such properties, self-assembly studies of artificial sequence-defined oligomers is of great interest. In this paper, we show the use of hydrophilic, lipophilic, aromatic and fluorophilic monomers to synthesize a large library of truly monodisperse sequence-defined block co-oligo(phosphodiester)s. Automated and accurate control over the sequence allowed to rationally study the degree of polymerisation, blocks ratio, chemical composition and orthogonal supramolecular interactions influence on self-assembly. Interestingly, our studies revealed remarkable morphological changes (spheres to nanosheets) caused by very small differences between polymers, e.g., polymers differing by a single monomer unit. Inverting block sequence in multi-block copolymers also caused a dramatic increase in micelle size. Conventional polymerization does not allow the exploration of these subtle variations in polymer sequence or composition. Therefore, fast synthesis and purification of a variety of oligomers with slightly different sequences allows studying the supramolecular chemistry of precision oligomers in a systematic way. It paves the way to the rational design of functional sequence-defined polymers.

Introduction

Nature uses sequence-defined polymers for molecular recognition, catalysis and information coding. DNA and proteins are biopolymers of specific lengths and sequences, allowing them to fold into highly functional macromolecules. To mimic such bio-macromolecules, many new synthetic routes have been developed in the past few years.[1,2] They rely on state-of-the-art polymerisation techniques,[3–5] biopolymer templated synthesis[6–8] or iterative strategies.[9–17] Among these, iterative approaches remain the method of choice to achieve the finest sequence-control. In particular, phosphoramidite chemistry on solid-phase has been shown to combine the advantages of high sequence precision,[16,18–20] high degree of polymerisation,[21] heterofunctional monomers,[22] and water solubility of the resulting oligo(phosphodiester)s.[23] Very high coupling yields and adequate purification result in monodisperse oligomers and polymers. In addition, this chemistry has been the method of choice to make oligonucleotides for decades, thus leading to cost-effectiveness and ready scale-up.[24] The ultimate goal with precision polymers is to mimic the efficiency and selectivity of biopolymers for example in catalysis. However, current applications remain limited mostly to digital storage.[25] It is necessary to provide insight into the self-assembly and folding aspects of sequence-defined oligomers in order to design functional precision macromolecules.

The self-assembly of block copolymers (BCPs) has been extensively investigated for numerous applications including drug delivery, nanolithography, photoactive structures and porous materials.[26] BCPs can self-assemble into a range of structures: from simple spherical micelles to semi-crystalline cylindrical structures, vesicles or nanosheets.[27–31] The latter allow the 2D organization of organic and inorganic molecules with applications ranging from catalytic arrays, semiconductor materials or solar cells.[32] Among BCPs, diblock copolymers (AB) have been the most studied, leading to a detailed understanding of their self-assembly by microphase separation between the blocks.[33] The degree of polymerisation (N), the volume fraction of each block (f) and the Flory-Huggins parameter (χ), representative of the degree of incompatibility of both blocks, were shown to influence the polymer assembly at equilibrium in a non-solvent for one of the blocks.

Due to the unique tunability of precision polymers, multiple orthogonal interactions can be engineered in a sequence defined manner. Much like protein folding, these orthogonal interactions

can result in controlled folding of single polymer chains and/or highly specific inter-chain assembly.[34] Therefore, assembly rules of sequence-defined oligomers combine those for block copolymers and those for single-chain folding. Systematic study of these rules would give important insight into the self-assembly of sequence-defined oligomers.

Herein, we report a method to readily synthesize sequence-defined block oligo(phosphodiester)s, rationally varying the three parameters (N, f_A and χ) shown to influence self-assembly of block copolymers. The automated synthetic strategy was key to simultaneously generate several sequences with different degree of polymerisation (N) and blocks ratio (f_A). Four hydrophilic, hydrophobic, aromatic and "fluorophilic" monomers were chosen in order to precisely engineer multiple orthogonal interactions in oligomers and vary the Flory-Huggins parameter (χ). A library of 15 monodisperse block-oligomers with various sizes and sequences was synthesized. Due to their anionic nature, they were easily purified and analyzed using methods that have been already developed for nucleic acids, such as gel electrophoresis. The oligomers self-assembled in magnesium containing buffers. Variation of monomer type, blocks ratio and length of the oligomers resulted in spherical micelles of different size and nanosheets. Interestingly, our studies revealed the dramatic morphological effect caused by very subtle differences like adding precisely one monomer on the oligomer chain. For example, adding a single naphthalene monomer unit on the same block co-oligomer chain changed the morphology from spheres to nanosheets, and inverting the sequence of two blocks on the same oligomer caused a dramatic increase in micelle size. A number of trends in precision oligo(phosphodiester)s self-assembly were deduced from this investigation. They highlight the valuable insights into supramolecular behaviour that can be obtained using sequence-defined oligomers.

Results and discussion

a. Phosphoramidite monomers from diols

We specifically chose four monomers that would allow us to engineer the hydrophobic effect, π-π stacking and the "fluorophilic" effect. The latter occurs when several perfluorocarbon chains show low affinity for surrounding molecules due to their amphiphobicity (ie hydrophobic and oleophobic). With a palette of these three interactions, we synthesized a variety of different nanostructures. A simple synthetic strategy based on diol precursors was used to produce the monomers in a cost-effective and scalable manner. First, the diols were converted into mono DMT-protected alcohol and then turned into phosphoramidites as shown on scheme 1. We believe a large variety of monomers can be conceivably made through this simple method. Our group previously reported the synthesis of sequence-controlled polymers appended to DNA using monomers **C12** (12 carbon alkyl chain) and **HEG** (hexaethylene glycol).[16] Both were made from diol precursors and DNA oligomers containing these moieties were shown to self-assemble in water.[18,35] We chose these two monomers as simple hydrophobic and hydrophilic units respectively. For π-π stacking, we chose a monomer (**NAP**) that contains a naphthalene moiety, made from a readily available diol precursor.[22] **NAP** also allows the oligomers to be UV-detectable, allowing their quantification through spectrophotometry. Finally, a fluorophilic monomer (**PFC)**[19] containing a perfluorocarbon chain was used. High efficiency couplings are achieved with **C12**, **HEG**, **NAP** and **PFC** showing that designing monomers using diols generally is an efficient strategy to generate sequence-controlled oligomers (Figure 1, Table 1).

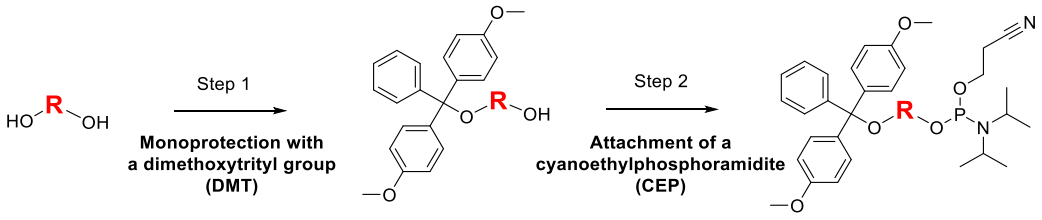

Scheme 1. General strategy to obtain a DNA synthesizer-compatible monomer from a diol.

b. Synthesis of sequence-defined block co-oligomers with a DNA synthesizer

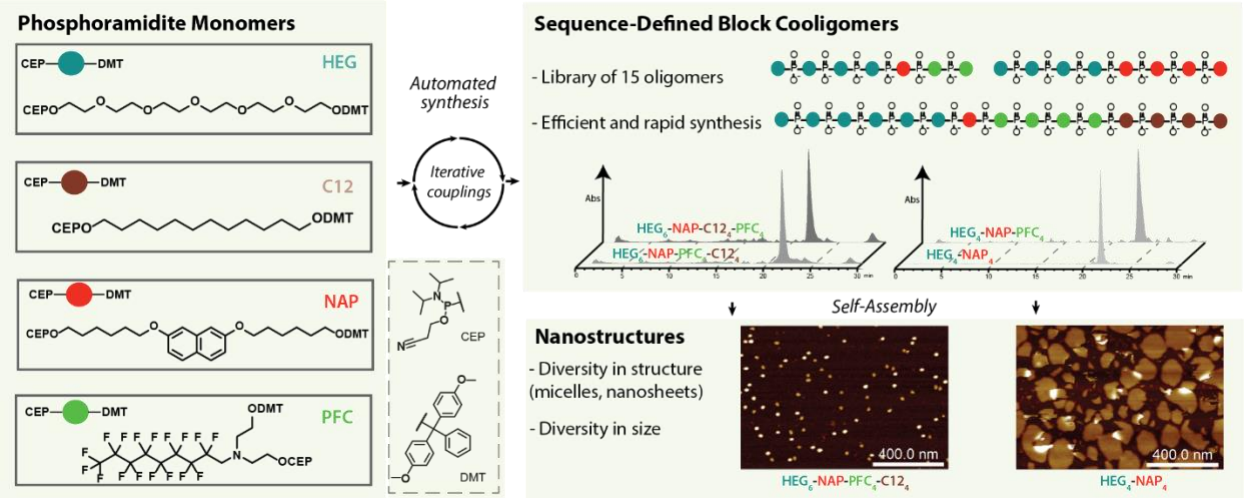

Figure 1. Strategy to obtain a library of nanostructures with different sizes and shapes from sequence-defined block co-oligomers made from 4 phosphoramidites and an automated DNA synthesizer. Chromatograms are from Reverse-Phase High Performance Liquid Chromatography (RP-HPLC) with detection at 260nm. Atomic Force Microscopy (AFM) images were obtained in Mg^{2+} containing buffer conditions. Full HPLC chromatograms and gradients as well as details on the AFM images are available in the supplementary information.

Monomers **HEG**, **C12**, **NAP** and **PFC** were used to rationally design a library of sequence-controlled oligomers with different sequences and degrees of polymerisation in an automated fashion (Figure 1). The four phosphoramidites were used in a standard DNA synthesizer along with commercially available DNA synthesis reagents. Coupling cycles were similar to DNA synthesis, but the coupling time was increased to 10 minutes and phosphoramidite concentration was kept at ca. 0.1M in dry dichloromethane. With full synthetic cycles of 15 minutes, the synthesis of a 10-mer takes no longer than 2h30min. Some polymers were made from a divergent method. For example, oligomers **A2** (**HEG_4-NAP_2**) and **A3** (**HEG_4-NAP_3**) were made from the same Controlled Pore Glass (CPG) support. After 4 coupling cycles with **HEG** and two with **NAP**, half of the CPG beads was deprotected and half of it underwent a last coupling cycle with a **NAP** unit. This divergent technique allowed to synthesize twice more oligomers. As a conclusion, considering the synthesizer preparation, handling of the CPG and deprotection (2h30 in a basic aqueous medium), the synthesis of a 15-member oligomer library shown here can take less than 9h with a common six ports MerMade® synthesizer. The phosphate groups of our polymers make

them water-soluble, enhancing their great ease of manipulation. Similarly to nucleic acids, they can be quantified easily using UV absorbance at 260 nm and the extinction coefficient of **NAP** (see SI-III). The first series of oligomers (**A**) (Table 1) shows the possibility of making diblock copolymers with varying length and hydrophilic/hydrophobic ratios with monomers **HEG** and **NAP**. For example, **A2** (**HEG**$_4$-**NAP**$_2$) and **A4** (**HEG**$_4$-**NAP**$_4$) have different lengths and ratios while **A4** (**HEG**$_4$-**NAP**$_4$) and **A7** (**HEG**$_6$-**NAP**$_6$) only differ by the degree of polymerisation. Another series (**B**) shows sequences with up to four different artificial monomers. While the A series involved more π-π stacking, the main supramolecular interactions for **B** oligomers are the hydrophobic and fluorophilic effect. For example, **B2** (**HEG**$_4$-**NAP**-**C12**$_4$) and **B4** (**HEG**$_4$-**NAP**-**PFC**$_4$**)** have similar length and sequence but the solvent incompatible block is mostly made of hydrophobic **C12** in one case and fluorophilic **PFC** units in the other. Synthesis of co-oligomers where fluorophilic, hydrophobic and π-π stacking should influence self-assembly was also achieved in high yields with **B5** (**HEG**$_6$-**NAP**-**PFC**$_4$-**C12**$_4$) and **B6** (**HEG**$_6$-**NAP**-**C12**$_4$-**PFC**$_4$).

C. Purification of sequence-defined block co-oligo(phosphodiester)s

All oligomers except **A8** were purified through reverse-phase high-performance liquid chromatography. Indeed, the addition of a hydrophobic phosphoramidite (**C12**, **NAP** or **PFC**) during the last coupling cycle led to a clear shift between the full-length product and the by-products on the chromatogram. Global yields were found to be very high in most cases (e.g. oligomer **B5**, 79% for the last 8 couplings meaning an average of 97% per coupling, table 1). Other types of sequence-defined polymers found in the literature are mostly isolated through reverse-phase HPLC.[11,12] However, this literature method is not adapted to hydrophilic or long oligomers. For example, in the case of oligomer **A8** (**NAP**$_8$-**HEG**$_{12}$), hydrophilic monomer **HEG** was added last. Thus, the full-length oligomer and the n-1 impurity (minus one **HEG** unit) would have similar retention times on a reverse-phase chromatogram. In the polymer chemistry field, Size Exclusion Chromatography (SEC) is used as a major characterization and sometimes purification method. However, in the case of sequence-defined polymers, the resolution achieved by SEC is not good enough to obtain good separation between a polymer and a n-1 impurity.[15] Our oligo(phosphodiester)s have the same anionic backbone as nucleic acids. Therefore, we tried to apply typical procedures used for DNA purification. Anionic exchange chromatography was considered but did not lead to satisfactory results in our case due to the oligomer self-assembly at high salt concentration. We also wanted to apply the "DMT-on" purification method. This strategy relies on leaving the hydrophobic DMT group on the last monomer added so that a clear shift is observed using reverse-phase chromatography. In the case of a model DNA 19mer with a DMT moiety at the 5' end, the DMT stayed on under usual HPLC conditions. However, it fell off from another strand modified at the 5' end with 6 **C12** and the final DMT group. Therefore, we believe this strategy is difficult to apply to a variety of oligomers (Figure S2).

We considered another classic method for DNA chemists more adapted to anionic oligomers: electrophoresis. This method was recently applied by Sutton et al. for the separation of oligo(acrylic acid)s through free solution capillary electrophoresis.[36] We observed that oligomers containing **NAP** could be visualized after running polyacrylamide gel electrophoresis (PAGE) and staining with GelRed®, a molecule used to stain DNA (Figure 2b). The cationic and aromatic GelRed® molecules most likely interact electrostatically with the anionic oligo(phosphodiester)s, and with **NAP** units via π-π stacking. This experiment showed clear electrophoretic mobility

differences between oligomers of different size and sequence. With oligo(phosphodiester)s, PAGE appeared as a way to differentiate oligomers similar in size. We believe it can be used more accurately than SEC. Oligomers **A6**, **A7** and **A8** were purified via PAGE. They were loaded and run on a 20% polyacrylamide gel and visualized with UV light (Figure 2c). Main bands were excised, extracted from the gel using the "crush and soak" technique (see SI-IV) and salt-purified using a small SEC filter. Hence, we showed that such polymers can be purified through gel electrophoresis due to their anionic nature leading to a truly monodisperse population of oligomers.

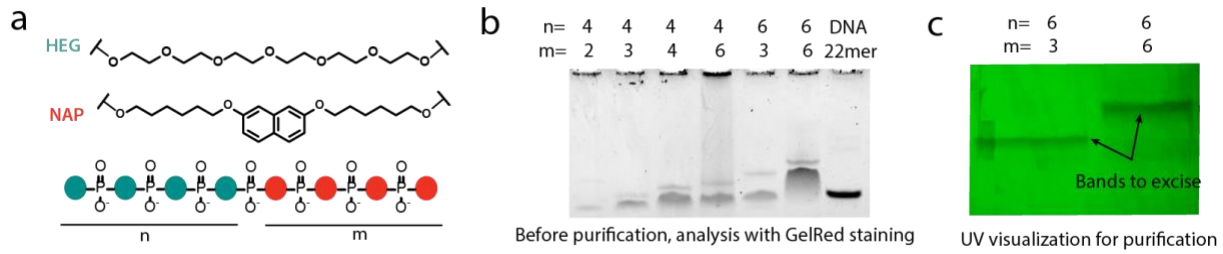

Figure 2. Description of the block co-oligomers (a), PAGE analysis (20% in denaturing conditions) of the crude mixtures of oligomers obtained after cleavage from solid support. Interestingly, **HEG$_4$-NAP$_6$** seems to self-assemble even in denaturing conditions (non-penetrating band). (b), Visualization of oligomers **A6** and **A7** through UV 254nm illumination of a 20% polyacrylamide gel on a fluorescent TLC plate (c).

d. Self-assembly characterization

Table 1. Yields and self-assembly characterization of oligomers made

Name	Sequence	HPLC Yields[a] (%)	Morphology in aqueous medium[b]	Hydrodynamic diameter[d] [nm]	Poly-Dispersity Index[c] [%]
A1	**HEG_4-NAP**	75	Unimers (D)	-[f]	-
A2	**HEG_4-NAP_2**	72	Unimers (D)	-[f]	-
A3	**HEG_4-NAP_3**	71	Spherical (A/D/G)	16.0	7.6
A4	**HEG_4-NAP_4**	91	Nanosheets (A/D/G)	109[g]	17.2
A5	**HEG_4-NAP_6**	41	Not determined	-[h]	-
A6	**HEG_6-NAP_3**	65	Spherical (D/G)	15.6	12.2
A7	**HEG_6-NAP_6**	44	Nanosheets (A/D/G)	50.0[g]	38.4
A8	**HEG_{12}-NAP_8**	-[e]	Spherical (A/D)	42.2	12.8
A9	**NAP_2-HEG_4-NAP_2**	48	Not determined	-[h]	-
B1	**HEG_4-$C12_4$-NAP**	86	Spherical (G)	-[h]	-
B2	**HEG_4-NAP-$C12_4$**	83	Spherical (G)	-[h]	-
B3	**HEG_6-NAP-$C12_4$**	87	Spherical (A/D/G)	13.2	7.8
B4	**HEG_4-NAP-PFC_4**	76	Spherical (G)	-[h]	-
B5	**HEG_6-NAP-PFC_4-$C12_4$**	79	Spherical (A/D/G)	17.4	13.2
B6	**HEG_6-NAP-$C12_4$-PFC_4**	70	Spherical (A/D/G)	21.6	15.8

a Yields were calculated through product peak area by RP-HPLC (260 nm detection) considering the relative absorbance of by-products. Yields could only be calculated from the first naphthalene introduction. b Methods of morphology determination is between parentheses. A=AFM, D=DLS, G=Gel electrophoresis. c Measured by DLS, 25 µM d Obtained from calculations using a globular protein model with Dynamics v.6.b e Yields could not be measured by HPLC since the **HEG** moieties were added after the **NAP** ones. f Results seem to show the presence of only very small particles (Figure S15). g. AFM studies show the presence of non-spherical objects in this case, hydrodynamic diameters are reported to give an insight into these structures size in solution. h. Over-scattering was observed.

The amphiphilic nature of our oligomers made them good candidates for self-assembly in aqueous solvents. Inspired by nucleic acids chemistry and by our previous work,[16] we decided to mainly study the self-assembly properties of our oligomers in magnesium containing buffers. Divalent magnesium cations interact with the phosphate negative charges minimizing repulsion between

anionic oligomers. This allows the formation of phosphate-containing hydrophobic cores.[16] Strikingly, the higher solubility of all oligomers **A** and **B** in water due to the phosphate groups allows them to directly self-assemble from the dry state to the aqueous state. To ensure clean self-assembly of our oligomers, we annealed them from 95 °C to 4 °C in 1 hour. Annealing prevents the formation of kinetically trapped nanostructures and favors the thermodynamic product. To characterize our structures, we performed Atomic Force Microscopy (AFM), Dynamic Light Scattering (DLS) and Agarose Gel Electrophoresis (AGE). AFM was performed in both dry and fluid conditions, using Nickel (II) to favour the interaction of the negatively charged phosphates with the mica (see SI-VI).[37] Under these conditions, AFM showed the formation of spherical micelles with six of the oligomers (Figures 3, S9, S11-S15).

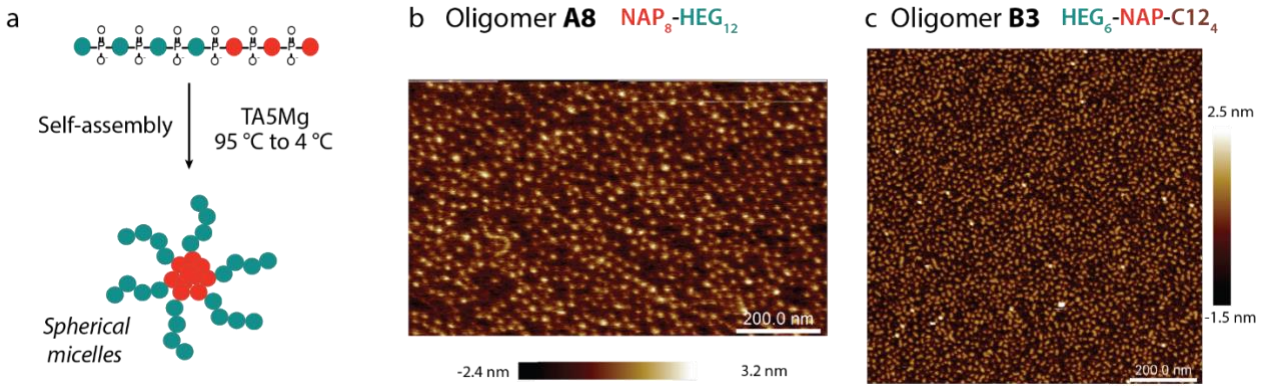

Figure 3. Schematic representation of spherical micelle self-assembly (a), Atomic Force Microscopy images on Mica of spherical micelles aggregates in dry conditions of **A8,** 10 µM (b) and in fluid conditions of **B3**, 50 µM (c).

On the other hand, two oligomers, **A4** (**HEG**$_4$-**NAP**$_4$) and **A7** (**HEG**$_6$-**NAP**$_6$), formed nanosheets of uniform height (Figures 4, S4-S8, S10). The average height in dry images was difficult to evaluate, as magnesium and nickel salt deposits resulted in a non-uniform background layer on mica. In liquid, the average height of **A4** is 5.7 nm. Low voltage Transmission Electron Microscopy (TEM) was also performed with **A4** (**HEG**$_4$-**NAP**$_4$). Uniform nanosheets were observed further confirming the assembly of **A4** into sheets when deposited on mica or carbon films (Figures 4c and S16). Sequence-defined peptoids and pyrene-based oligo(phosphodiester)s nanosheets have attracted significant interest due to potential applications in organic materials

templated growth.[38,39] However, examples of sequence-defined nanosheets are rare and usually involve only rigid monomers and very short sequences. In our case, the possibility of making such sheets in the presence of the flexible **HEG** corona highlights the great stability of the sheets core.

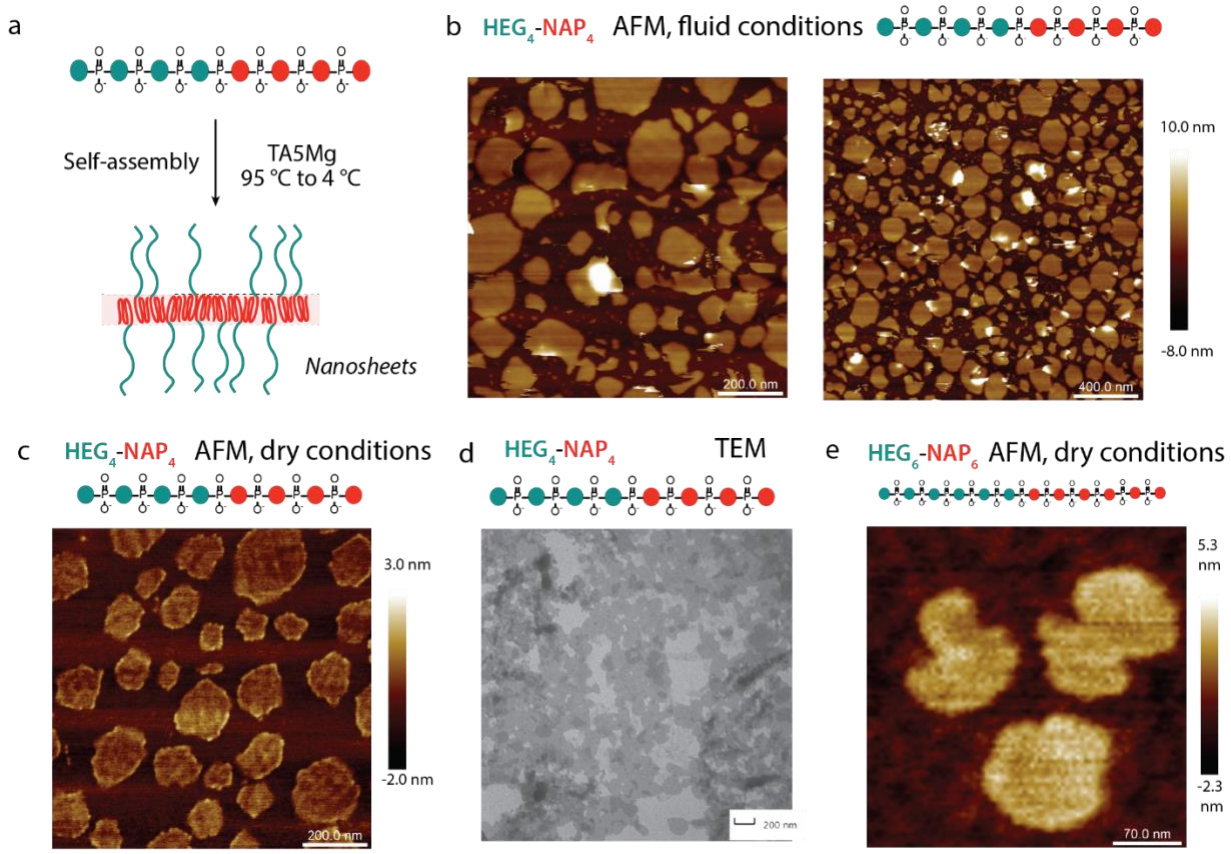

Figure 4. Schematic representation of spherical micelle self-assembly (a), Atomic Force Microscopy images on Mica of nanosheet forming structures with **HEG$_4$-NAP$_4$** (oligomer **A4**) in fluid conditions (b), in dry conditions (c), using Low-Voltage Electron Miscroscopy (LVEM) in a transmission mode (d) and Atomic Force Microscopy images on Mica of nanosheet forming structures with **HEG$_6$-NAP$_6$** (oligomer **A7**) in dry conditions (e). Concentration used is 50 µM.

To study our oligomers in solution, we also performed Dynamic Light Scattering (DLS) measurements. The technique allowed us to estimate the diffusion coefficient and the polydispersity index of our structures (SI-VIII). Most spherical micelle forming oligomers led to signals confirming the self-assembly into discrete highly monodisperse nanostructures. Hydrodynamic diameters (Table 1) were calculated using a globular protein model. This gives a

good estimation of the size of the spherical micelles in solution (see section e for analysis). As expected, nanosheet forming structures had a greater polydispersity index and a smaller diffusion coefficient than the other structures. **A1** (**HEG$_4$-NAP**) and **A2** (**HEG$_4$-NAP$_2$**) had similar signal as the buffer control, showing that they do not self-assemble under the conditions explored (Figure S15). Over-scattering was often observed in the case of **A5** (**HEG$_4$-NAP$_6$**), **A9** (**NAP$_2$-HEG$_4$-NAP$_2$**), **B1** (**HEG$_4$-C12$_4$-NAP)**, **B2 (HEG$_4$-NAP-C12$_4$-NAP)** and **B4 (HEG$_4$-NAP-PFC$_4$)**. We believe their self-assembly may induce the formation of some large aggregates at the concentration (25 µM) used for DLS.

Inspired by our expertise in nucleic acid characterization, we also used Agarose Gel Electrophoresis (AGE) to gather more information about our oligomer self-assembly. Indeed, agarose gels have larger pore size than polyacrylamide gels allowing larger constructs such as self-assembled structures to go through the gel. In the case of the library of oligomers that we describe here, diblock oligomers **A3** (**HEG$_4$-NAP$_3$**), **A6** (**HEG$_6$-NAP$_3$**) as well as **B1 (HEG$_4$-C12$_4$-NAP)** to **B6** (**HEG$_6$-NAP-C12$_4$-PFC$_4$)** have similar mobility behavior as DNA-polymer micelles reported by our group elsewhere[19] (Figure 5 and S19) which is in accordance with the AFM and DLS results. Oligomers **A4** (**HEG$_4$-NAP$_4$**), **A5** (**HEG$_4$-NAP$_6$**) and **A7** (**HEG$_6$-NAP$_6$**) do not show discrete bands on these gels but smearing bands or non-penetrating material. This observation is consistent with the sheets[40] observed by AFM and TEM for **A4** and **A7**. Hence, AGE is a valuable inexpensive method to qualitatively characterize the self-assembly behavior of various nanostructures at once. This is of great interest for relating the influence of degree of polymerisation, sequence and chemical composition with self-assembly.

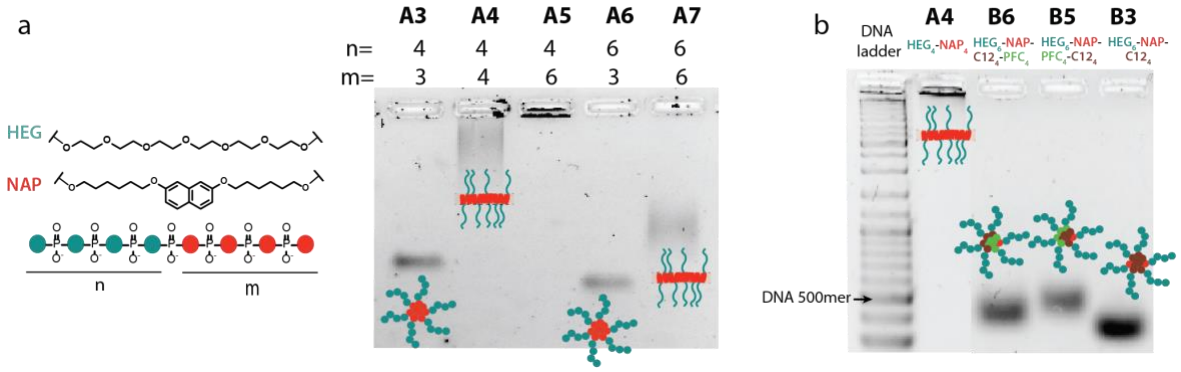

Figure 5. AGE with sequence-defined block co-oligomers in native conditions in large pores agarose gel (2.5%). Diblock oligomers (a) and B series of oligomers (b). The DNA ladder shows that some structures move as fast as a 500mer double-stranded DNA.

e. Influence of sequence on self-assembly

Taken together, our results can lead to multiple conclusions regarding the influence of parameters such as size, composition and supramolecular interactions involved in the self-assembly of sequence-defined oligomers. **A1** (**HEG**$_4$-**NAP**) to **A5** (**HEG**$_4$-**NAP**$_6$) were designed to gradually increase the hydrophobic content and π-π stacking interactions while keeping the hydrophilic part constant. This series shows the potential of precision polymers, which allow the systematic analysis of very subtle differences of single monomer units between oligomers. We showed through Dynamic Light Scattering that **A1** and **A2** do not self-assemble. This result was expected considering their very low hydrophobic content. With one additional **NAP** monomer, spherical micelles with a **NAP**-containing core and a **HEG** corona are now formed. **A2** and **A3** only differ by one **NAP** monomer. This small difference triggered self-assembly into spherical micelles as shown by AFM, DLS and AGE. Interestingly, adding another **NAP** monomer radically changes the mode of assembly of the oligomer: nanosheets were observed on mica with AFM and on graphene films with TEM. DLS and AGE also suggest the formation of higher-order structures. This result is in accordance with the subtle **NAP**/**HEG** ratio increase from **A3** (3:4) to **A4** (4:4). This drastic change in assembly between two similar oligomers is striking, compared to conventional BCPs. In the case of sequence-defined oligomers, only one monomer can trigger self-assembly from spherical micelles to nanosheets.

A6 (**HEG**$_6$-**NAP**$_3$) was designed to have similar hydrophobic content as **A3** (**HEG**$_4$-**NAP**$_3$) but two more hydrophilic **HEG** units. We hypothesized that **A6** would form spherical micelles with a larger hydrophilic corona. However, DLS and AGE seem to show that **A6** micelles is comparable or even smaller in size than **A3**, suggesting that **A6** assembles with a denser chain-packing than **A3**. On the other hand, **A8** (**HEG**$_{12}$-**NAP**$_8$) was designed to have a similar **HEG** to **NAP** ratio than **A3** but a higher degree of polymerization. We observed that both oligomers form spherical micelles, but the diameter of **A8** is much larger than **A3**. In other words, a small increase in hydrophilic content did not lead to a micelle diameter increase, but a higher degree of polymerization led to larger micelles.

In the case of nanosheets, **A4** (**HEG**$_4$-**NAP**$_4$) and **A7** (**HEG**$_6$-**NAP**$_6$) have the same HEG:NAP ratio, and only differ by their degree of polymerization. As expected, they formed similar lamellae

structures. However, contrary to the case of **A8** and **A3**, the higher DP nanostructures have a larger diffusion coefficient (SI), implying that **A7** forms smaller structures than **A4**.

The **B** series of oligomers was designed to gather information on the influence of different supramolecular interactions on self-assembly. We could change the type of interaction by changing the nature of the monomers involved. For example, **B2** (**HEG$_4$-NAP-C12$_4$**) and **B4** (**HEG$_4$-NAP-PFC$_4$**) differ by the type of monomers involved but have similar degrees of polymerization. Using AGE, **B2** appears to have a smaller size than **B4** (Figure S21), possibly indicating that using **PFC** leads to larger micelles than **C12**.

We designed **B5** (**HEG$_6$-NAP-PFC$_4$-C12$_4$**) and **B6** (**HEG$_6$-NAP-C12$_4$-PFC$_4$**) because lipophilic and fluorophilic triblocks copolymers can sometimes induce unusual morphologies as reported elsewhere.[41] In our case, AFM and DLS results show the presence of spherical micelles (Figure 1 and S12-S13). The significant diameter difference of **B5** (**HEG$_6$-NAP-PFC$_4$-C12$_4$**) (17.4 nm) and **B6** (**HEG$_6$-NAP-C12$_4$-PFC$_4$**) (21.6 nm) observed by DLS in solution highlights the crucial role of the oligomer sequence. Indeed, these two oligomers have similar degree of polymerisation and composition but the fluorophilic and lipophilic blocks positions are inverted.

Through the design and synthesis of oligomers **A** and **B**, we observed self-assembly trends depending on the size, blocks ratio, blocks position and monomer nature of each oligomer. Some parameters dictated very different behaviours. For example, oligomers **A3** (**HEG$_4$-NAP$_3$**) and **A4** (**HEG$_4$-NAP$_4$**) only differ by one monomer but have radically different modes of assembly. These conclusions give insight into the self-assembly of oligo(phosphodiester)s and can be used to rationally design nanostructures for specific applications.

Conclusions

In conclusion, we demonstrated the rapid synthesis of a new class of self-assembling sequence-defined block oligomers with rational variation of the degree of polymerisation – i.e., increasing the number of monomers one by one in a monodisperse chain, block ratio, monomer type and supramolecular interactions. We designed four monomers to introduce hydrophobic and fluorophilic effects as well as π-π stacking in the final oligomers. Purification was achieved using reverse-phase chromatography or simple electrophoresis techniques. Block co-oligomers obtained

were truly monodisperse. Self-assembly experiments revealed the formation of spherical micelles of different sizes as well as two-dimensional nanosheets. For a given oligomer, our observations were systematically compared to the ones obtained with oligomers of different length, sequence or chemical composition. They revealed how these parameters influenced the constructs size and modes of assembly. Perfect sequence- and length-control was found to be a determinant parameter in the self-assembly process. Indeed, a small modification in the sequence can have a drastic effect in the nanostructure output (size or shape).

Automated synthesis provides the possibility to rationally study new parameters in block copolymer assembly, such as addition of a single monomer to a chain, or inversion of polymer sequence. It can significantly broaden our understanding of sequence-defined oligomers and paves the way to the design of functional precision polymers.

Conflicts of interest

The authors declare no conflict of interest.

Supporting Information

Electronic Supplementary Information (ESI) available: detailed synthetic and purification protocols, additional characterization data (HPLC, MS, DLS, gel electrophoresis, AFM, TEM).

Acknowledgements

The authors thank NSERC, CIHR, FRQNT, the Canada Research Chairs program, the Qatar National Research Fund (QNRF, project number NPRP 5 - 1505 - 1 – 250) for support. D. de Rochambeau thanks NSERC for a CREATE training program in Bionanomachines (CTPB) scholarship. We thank Dr. Alexander Wahba for his help with MS characterization, Dr. Kai Lin Lau and Xin Luo for imaging the structures with high-voltage TEM.

References

(1) Solleder, S. C.; Schneider, R. V.; Wetzel, K. S.; Boukis, A. C.; Meier, M. A. R. Recent Progress in the Design of Monodisperse, Sequence-Defined Macromolecules. *Macromol. Rapid Commun.* **2017**, *38* (9), 1600711.

(2) Szymański, J. K.; Abul-Haija, Y. M.; Cronin, L. Exploring Strategies to Bias Sequence in Natural and Synthetic Oligomers and Polymers. *Acc. Chem. Res.* **2018**, *51* (3), 649–658.

(3) Gutekunst, W. R.; Hawker, C. J. A General Approach to Sequence-Controlled Polymers Using Macrocyclic Ring Opening Metathesis Polymerization. *J. Am. Chem. Soc.* **2015**, *137* (25), 8038–8041.

(4) Lawrence, J.; Lee, S.-H.; Abdilla, A.; Nothling, M. D.; Ren, J. M.; Knight, A. S.; Fleischmann, C.; Li, Y.; Abrams, A. S.; Schmidt, B. V. K. J.; et al. A Versatile and Scalable Strategy to Discrete Oligomers. *J. Am. Chem. Soc.* **2016**, *138* (19), 6306–6310.

(5) Ogura, Y.; Artar, M.; Palmans, A. R. A.; Sawamoto, M.; Meijer, E. W.; Terashima, T. Self-Assembly of Hydrogen-Bonding Gradient Copolymers: Sequence Control via Tandem Living Radical Polymerization with Transesterification. *Macromolecules* **2017**, *50* (8), 3215–3223.

(6) Kleiner, R. E.; Brudno, Y.; Birnbaum, M. E.; Liu, D. R. DNA-Templated Polymerization of Side-Chain-Functionalized Peptide Nucleic Acid Aldehydes. *J. Am. Chem. Soc.* **2008**, *130* (14), 4646–4659.

(7) Niu, J.; Hili, R.; Liu, D. R. Enzyme-Free Translation of DNA into Sequence-Defined Synthetic Polymers Structurally Unrelated to Nucleic Acids. *Nat. Chem.* **2013**, *5* (4), 282–292.

(8) Milnes, P. J.; McKee, M. L.; Bath, J.; Song, L.; Stulz, E.; Turberfield, A. J.; O'Reilly, R. K. Sequence-Specific Synthesis of Macromolecules Using DNA-Templated Chemistry. *Chem. Commun. (Camb).* **2012**, *48* (45), 5614–5616.

(9) Barnes, J. C.; Ehrlich, D. J. C.; Gao, A. X.; Leibfarth, F. A.; Jiang, Y.; Zhou, E.; Jamison, T. F.; Johnson, J. A. Iterative Exponential Growth of Stereo- and Sequence-Controlled Polymers. *Nat. Chem.* **2015**, *7* (10), 810–815.

(10) Lewis, J. E. M.; Winn, J.; Cera, L.; Goldup, S. M. Iterative Synthesis of Oligo[*n*]Rotaxanes in Excellent Yield. *J. Am. Chem. Soc.* **2016**, *138* (50), 16329–16336.

(11) Grate, J. W.; Mo, K.-F.; Daily, M. D. Triazine-Based Sequence-Defined Polymers with Side-

Chain Diversity and Backbone-Backbone Interaction Motifs. *Angew. Chem. Int. Ed. Engl.* **2016**, *55* (12), 3925–3930.

(12) Martens, S.; Van den Begin, J.; Madder, A.; Du Prez, F. E.; Espeel, P. Automated Synthesis of Monodisperse Oligomers, Featuring Sequence Control and Tailored Functionalization. *J. Am. Chem. Soc.* **2016**, *138* (43), 14182–14185.

(13) Solleder, S. C.; Zengel, D.; Wetzel, K. S.; Meier, M. A. R. A Scalable and High-Yield Strategy for the Synthesis of Sequence-Defined Macromolecules. *Angew. Chem. Int. Ed. Engl.* **2016**, *55* (3), 1204–1207.

(14) Knight, A. S.; Zhou, E. Y.; Francis, M. B.; Zuckermann, R. N. Sequence Programmable Peptoid Polymers for Diverse Materials Applications. *Adv. Mater.* **2015**, *27* (38), 5665–5691.

(15) Al Ouahabi, A.; Charles, L.; Lutz, J.-F. Synthesis of Non-Natural Sequence-Encoded Polymers Using Phosphoramidite Chemistry. *J. Am. Chem. Soc.* **2015**, *137* (16), 5629–5635.

(16) Edwardson, T. G. W.; Carneiro, K. M. M.; Serpell, C. J.; Sleiman, H. F. An Efficient and Modular Route to Sequence-Defined Polymers Appended to {DNA}. *Angew. Chem. Int. Ed. Engl.* **2014**, *53* (18), 4567–4571.

(17) Kanasty, R. L.; Vegas, A. J.; Ceo, L. M.; Maier, M.; Charisse, K.; Nair, J. K.; Langer, R.; Anderson, D. G. Sequence-Defined Oligomers from Hydroxyproline Building Blocks for Parallel Synthesis Applications. *Angew. Chemie Int. Ed.* **2016**, *55* (33), 9529–9533.

(18) Chidchob, P.; Edwardson, T. G. W.; Serpell, C. J.; Sleiman, H. F. Synergy of Two Assembly Languages in DNA Nanostructures: Self-Assembly of Sequence-Defined Polymers on DNA Cages. *J. Am. Chem. Soc.* **2016**, *138* (13), 4416–4425.

(19) de Rochambeau, D.; Barłóg, M.; Edwardson, T. G. W.; Fakhoury, J. J.; Stein, R. S.; Bazzi, H. S.; Sleiman, H. F. "DNA–Teflon" Sequence-Controlled Polymers. *Polym. Chem.* **2016**, *7* (31), 4998–5003.

(20) König, N. F.; Al Ouahabi, A.; Poyer, S.; Charles, L.; Lutz, J.-F. A Simple Post-Polymerization Modification Method for Controlling Side-Chain Information in Digital Polymers. *Angew. Chemie Int. Ed.* **2017**, *56* (25), 7297–7301.

(21) Ouahabi, A. Al; Kotera, M.; Charles, L.; Lutz, J.-F. Synthesis of Monodisperse Sequence-Coded Polymers with Chain Lengths above DP100. *ACS Macro Lett.* **2015**, *4* (10), 1077–1080.

(22) De Rochambeau, D.; Sun, Y.; Barlog, M.; Bazzi, H. S.; Sleiman, H. F. Modular Strategy to Expand the Chemical Diversity of DNA and Sequence-Controlled Polymers. *J. Org. Chem.* **2018**, *83* (17), 9774–9786.

(23) Appukutti, N.; Serpell, C. J. High Definition Polyphosphoesters: Between Nucleic Acids and Plastics. *Polym. Chem.* **2018**, *9* (17), 2210–2226.

(24) Kosuri, S.; Church, G. M. Large-Scale de Novo DNA Synthesis: Technologies and Applications. *Nat Meth* **2014**, *11* (5), 499–507.

(25) Meier, M. A. R.; Barner-Kowollik, C. A New Class of Materials: Sequence-Defined Macromolecules and Their Emerging Applications. *Adv. Mater.* **2019**, 1806027.

(26) Schacher, F. H.; Rupar, P. A.; Manners, I. Functional Block Copolymers: Nanostructured Materials with Emerging Applications. *Angew. Chemie Int. Ed.* **2012**, *51* (32), 7898–7921.

(27) Chen, M.; Gothelf, K. V. Labeling of DNA via Rearrangement of S-2-Aminoethyl Phosphorothioates to N-(2-Mercaptoethyl)Phosphoramidates. *Org. Biomol. Chem.* **2008**, *6* (5), 908–911.

(28) Figg, C. A.; Carmean, R. N.; Bentz, K. C.; Mukherjee, S.; Savin, D. A.; Sumerlin, B. S. Tuning Hydrophobicity To Program Block Copolymer Assemblies from the Inside Out. *Macromolecules* **2017**, *50* (3), 935–943.

(29) Chavis, M. A.; Smilgies, D.-M.; Wiesner, U. B.; Ober, C. K. Widely Tunable Morphologies in Block Copolymer Thin Films Through Solvent Vapor Annealing Using Mixtures of Selective Solvents. *Adv. Funct. Mater.* **2015**, *25* (20), 3057–3065.

(30) Liu, N.; He, Q.; Wang, Y.; Bu, W. Stepwise Self-Assembly of a Block Copolymer–platinum(Ii) Complex Hybrid in Solvents of Variable Quality: From Worm-like Micelles to Free-Standing Sheets to Vesicle-like Nanostructures. *Soft Matter* **2017**, *13* (27), 4791–4798.

(31) Brendel, J. C.; Schacher, F. H. Block Copolymer Self-Assembly in Solution-Quo Vadis? *Chem. - An Asian J.* **2018**, *13* (3), 230–239.

(32) Govindaraju, T.; Avinash, M. B. Two-Dimensional Nanoarchitectonics: Organic and Hybrid Materials. *Nanoscale* **2012**, *4* (20), 6102.

(33) Mai, Y.; Eisenberg, A. Self-Assembly of Block Copolymers. *Chem. Soc. Rev.* **2012**, *41* (18), 5969.

(34) Lutz, J.-F.; Lehn, J.-M.; Meijer, E. W.; Matyjaszewski, K. From Precision Polymers to Complex

Materials and Systems. *Nat. Rev. Mater.* **2016**, *1*, 16024.

(35) Serpell, C. J.; Edwardson, T. G. W.; Chidchob, P.; Carneiro, K. M. M.; Sleiman, H. F. Precision Polymers and 3D DNA Nanostructures: Emergent Assemblies from New Parameter Space. *J. Am. Chem. Soc.* **2014**, *136* (44), 15767–15774.

(36) Sutton, A. T.; Arrua, R. D.; Gaborieau, M.; Castignolles, P.; Hilder, E. F. Characterization of Oligo(Acrylic Acid)s and Their Block Co-Oligomers. *Anal. Chim. Acta* **2018**, *1032*, 163–177.

(37) Pastré, D.; Piétrement, O.; Fusil, S.; Landousy, F.; Jeusset, J.; David, M.-O.; Hamon, L.; Le Cam, E.; Zozime, A. Adsorption of DNA to Mica Mediated by Divalent Counterions: A Theoretical and Experimental Study. *Biophys. J.* **2003**, *85* (4), 2507–2518.

(38) Robertson, E. J.; Battigelli, A.; Proulx, C.; Mannige, R. V.; Haxton, T. K.; Yun, L.; Whitelam, S.; Zuckermann, R. N. Design, Synthesis, Assembly, and Engineering of Peptoid Nanosheets. *Acc. Chem. Res.* **2016**, *49* (3), 379–389.

(39) Vybornyi, M.; Rudnev, A.; Häner, R. Assembly of Extra-Large Nanosheets by Supramolecular Polymerization of Amphiphilic Pyrene Oligomers in Aqueous Solution. *Chem. Mater.* **2015**, *27* (4), 1426–1431.

(40) Bousmail, D.; Chidchob, P.; Sleiman, H. F. Cyanine-Mediated DNA Nanofiber Growth with Controlled Dimensionality. *J. Am. Chem. Soc.* **2018**, *140* (30), 9518–9530.

(41) Holder, S. J.; Sommerdijk, N. A. J. M. New Micellar Morphologies from Amphiphilic Block Copolymers: Disks, Toroids and Bicontinuous Micelles. *Polym. Chem.* **2011**, *2* (5), 1018.